Supporting Information

Modulating the Supramolecular Helicity of Poly(m-phenylenediamine) by Achiral Monomer Copolymerization

Xinlin Zha, Guilin Xu, Yi Xiong, Zhong Yan, Ke Liu, Mufang Li, Yuanli Chen,* Jing Lu,* and Dong Wang*

Key Laboratory of Textile Fiber and Products (Wuhan Textile University), Ministry of Education, Wuhan Textile University, Wuhan, 430200, China.

*Corresponding authors's E-mail: chenyuanli2015@126.com, wangdon08@126.com and jlu@wtu.edu.cn.

Methods

Materials

M-phenylenediamine, p-phenylenediamine, diaminopyridines, aminopyridines, 2,2'-bipyridine, 4,4'-bipyridine, 2-amino-6-methylpyridine, m-phthalaldehyde, terephthalaldehyde and 2,6-diaminotoluene were obtained from Aladdin Industrial Corporation. Methylanilines, pyrrole, aniline, 3-amniophenol, formalin (37 wt%), glyoxal (40 wt%), glutaraldehyde (25 wt%), ammonium persulfate, anhydrous ethanol, methanol, acetonitrile, dimethyl sulfoxide, and pyrrole were purchased from Sinopharm Chemical Reagent Co.Ltd. All chemicals were used without further purification. The template molecule L/D-PhgC_{16} was synthesised based on our previous work.[1] Laboratory home-made deionized water (18.2 MΩ cm) was used for all experiments.

Characterization of D-PhgC_{16} and L-PhgC_{16} template molecules

D-PhgC_{16} ^{1}H NMR (600 MHz, DMSO-d_6, TMS, 25 °C): δ 8.45 (d, J = 7.2 Hz, 1H; CO<u>NH</u>CH), 7.37–7.27 (m, 5H; Ph), 5.29 (d, J = 7.8 Hz, 1H; NH<u>CH</u>COOH), 2.16 (t, J = 7.2 Hz, 2H; CH_2<u>CH_2</u>CONH), 1.48-1.44 (m, 2H; <u>CH_2</u>CH_2CONH), 1.27-1.21 (m, 24H; alkyl), 0.84 (t, J = 6.9 Hz, 3H). HRMS (Aglient 7250& JEOL-JMS-T100LP AccTOF) m/z $[M+H]^+$, calculated: 390.30027; found: 390.29979.

L-PhgC_{16} ^{1}H NMR (600 MHz, DMSO-d_6, TMS, 25 °C): δ 8.51 (d, J = 7.2 Hz, 1H; CO<u>NH</u>CH), 7.38–7.24 (m, 5H; Ph), 5.32 (d, J = 7.8 Hz, 1H; NH<u>CH</u>COOH), 2.16 (t, J = 7.2 Hz, 2H; CH_2<u>CH_2</u>CONH), 1.49-1.44 (m, 2H; <u>CH_2</u>CH_2CONH), 1.26-1.21 (m, 24H; alkyl), 0.84 (t, J = 7.2 Hz, 3H). HRMS (Aglient 7250& JEOL-JMS-T100LP AccTOF) m/z $[M+H]^+$, calculated: 390.30027; found: 390.30057.

Preparation of left-handed helical polypyrrole using D-PhgC$_{16}$ as the template molecule.

First, 0.050 mmol D-PhgC$_{16}$, 0.075 mmol 2,6-diaminopyridine and 1.44 mmol pyrrole were dissolved in a mixture of dimethyl sulfoxide (2 ml) and acetonitrile (4 ml), and then 30 ml of deionized water was added under stirring at room temperature. After stirring for 15 min, 1.52 mmol of ammonium persulfate (dissolved in 5 ml of H_2O) was added to induce the copolymerization. The reaction lasted for two hours and the solid products were collected by vacuum filtration. The obtained products were extracted in hot ethanol for at least 24h to remove template molecules and inorganic salts.

Preparation of left-handed helical polyaniline using D-PhgC$_{16}$ as the template molecule.

First, 0.050 mmol D-PhgC$_{16}$, 0.075 mmol 2,6-diaminopyridine and 1.09 mmol aniline were dissolved in a mixture of dimethyl sulfoxide (2 ml) and acetonitrile (4 ml), and then 30 ml of deionized water was added under stirring at room temperature. After stirring for 15 min, 1.17 mmol of ammonium persulfate (dissolved in 5 ml of H_2O) was added to induce the copolymerization. The reaction lasted for two hours and the solid products were collected by vacuum filtration. The obtained products were extracted in hot ethanol for at least 24h to remove template molecules and inorganic salts.

Preparation of left-handed helical copolymers of poly(m-phenylenediamine-*co*-pyrrole) using D-PhgC$_{16}$ as the template molecule.

First, 0.050 mmol D-PhgC$_{16}$, 0.075 mmol 2,6-diaminopyridine, 0.66 mmol m-phenylenediamine and 0.72 mmol pyrrole were dissolved in a mixture of dimethyl sulfoxide (2 ml) and acetonitrile (4 ml), and then 30 ml of deionized water was added under stirring at room temperature. After stirring for 15 min, 1.46 mmol of ammonium persulfate (dissolved in 5 ml of H_2O) was added to induce the copolymerization. The reaction lasted for two hours and the solid products were collected by vacuum filtration. The obtained products were extracted in hot ethanol for at least 24h to remove template molecules and inorganic salts.

Preparation of left-handed helical amine-aldehyde condensation-based polymers using D-PhgC$_{16}$ as the template molecule.

We take the p-phenylenediamine-formaldehyde system as a representative example to clarify. Briefly, 0.050 mmol D-PhgC$_{16}$, 0.075 mmol 2,6-diaminopyridine, and 1.36

mmol p-phenylenediamine were dissolved in a mixture of dimethyl sulfoxide (2 ml) and acetonitrile (4 ml), and then 30 ml of deionized water was added under stirring at room temperature. After stirring for 15 min, 1.96 mmol of aqueous formaldehyde was added to induce the copolymerization. The reaction lasted for two hours and the solid products were collected by vacuum filtration. The obtained products were extracted in hot ethanol for at least 24h to remove template molecules. For other amine- aldehyde condensation systems, only the amount of active monomer was changed while other conditions remained the same. For the 3-aminophenol-terephthalaldehyde system, 3-aminophenol was 1.00 mmol and terephthalaldehyde was 1.12 mmol. For the m-phenylenediamine-formaldehyde system, m-phenylenediamine was 1.36 mmol and formaldehyde was 1.96 mmol. For the m-phenylenediamine-glyoxal system, m-phenylenediamine was 1.00 mmol and glyoxal was 1.30 mmol. For the m-phenylenediamine-glutaraldehyde system, m-phenylenediamine was 1.00 mmol and glutaraldehyde was 0.64 mmol. For the m-phenylenediamine and m-phthalaldehyde system, m-phenylenediamine was 1.00 mmol and glutaraldehyde was 1.00 mmol.

Density functional theory (DFT) calculations

In order to reveal the packing mode for D-PhgC_{16}/MPD and D-PhgC_{16}/2,6-DAP systems, DFT investigations were performed using B3LYP functional and 6-31G(d) basis set. All optimization and frequency calculations were carried out with Gaussian 16 software. Considering the compute resource and time, two D-PhgC_{16}/MPD and two D-PhgC_{16}/2,6-DAP were selected in our study.

Characterization and measurements

1. SEM images were conducted on a JEOL-7800F field-emission scanning electron microscope. The acceleration voltage was 10 kV. Before testing, all samples were covered with platinum to improve its conductivity.

2. TEM images were performed with an FEI TECNAI G2 electron microscope. The operated voltage was 200 kV. TEM copper grids were used in all cases.

3. Thermogravimetric analysis (NETZSCH, TG209F3) was carried out at a heating rate of 10 °C/min from 30℃ to 800 °C.

4. XPS analysis was taken on an ESCALAB Xi+ instrument (Thermo Fischer, USA). The excitation source was Al Ka radiation with energy of 1486.6 eV.

5. ^{1}H NMR spectra were recorded on a Bruker Avance NEO (600 MHz) apparatus at

25 °C and the solvent used was DMSO-d_6.

6. High Resolution Mass spectra were recorded on an Aglient 7250& JEOL-JMS-T100LP AccuTOF instrument.

6. FTIR spectra were performed on a Bruker Tensor27 apparatus. The measurement wavenumbers were all between 400 and 4000 cm^{-1}.

7. XRD patterns were observed on a Rigaku Ultimate IV diffractometer, using Cu Ka radiation (λ=1.5418 A). All tests were recorded in step-scan mode.

8. DRCD and DRUV-vis spectra were carried out on a JASCO J-1500 CD spectrometer equipped with a DRCD device. The bandwidth and scanning speed were 5 nm and 200 nm/min, respectively.

Supplementary Figures

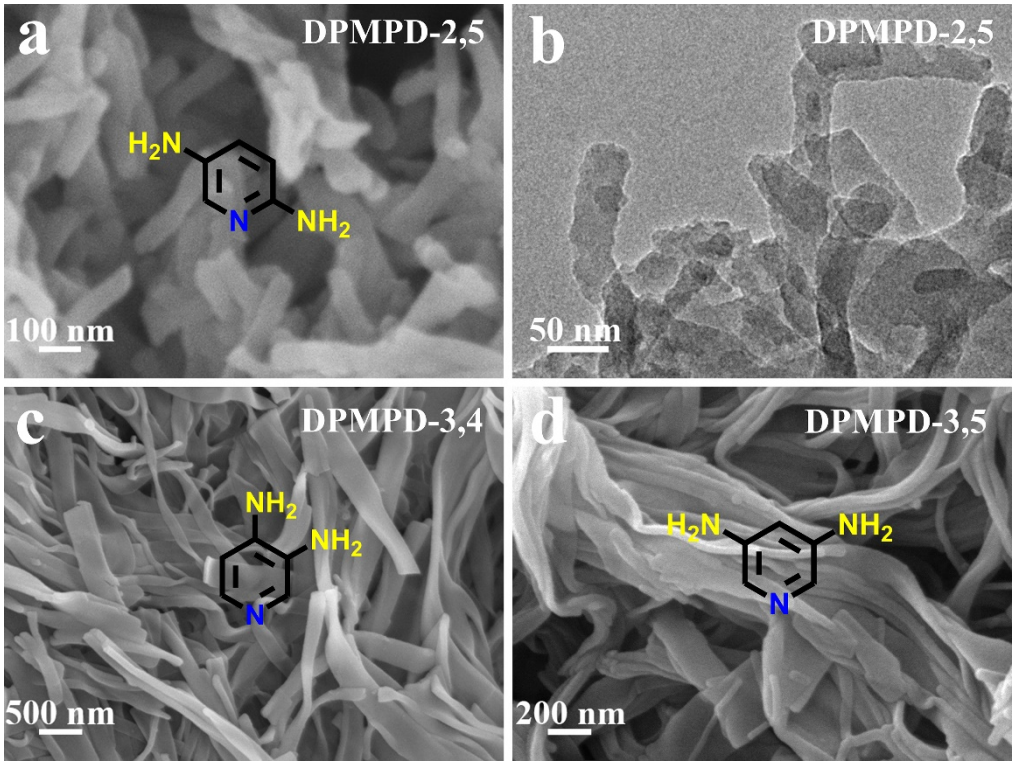

Fig. S1 (a) SEM image and (b) TEM image of DPMPD-2,5. SEM images of (c) DPMPD-3,4, (d) DPMPD-3,5.

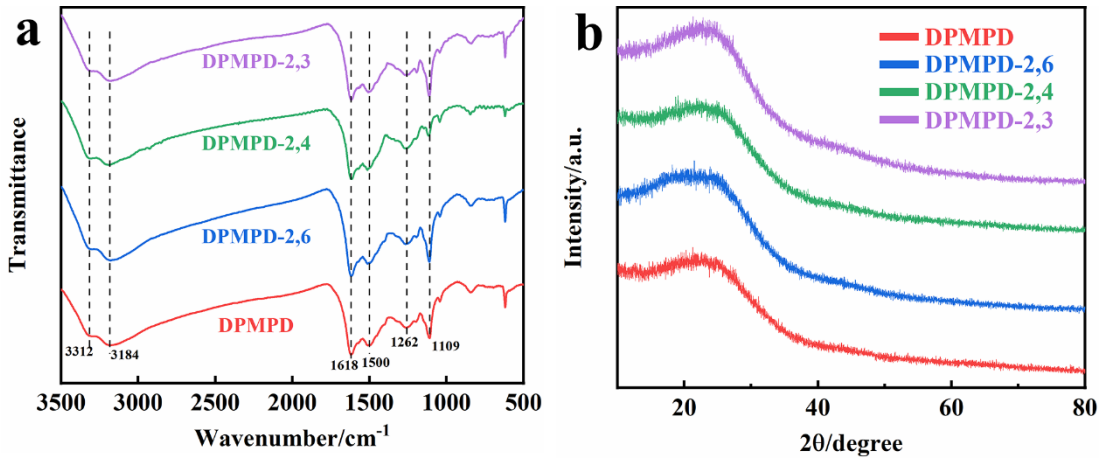

111

112 **Fig. S2** (a) FTIR spectra and (b) Wide-angle X-ray diffractogram patterns of DPMPD-based polymers.
113 (DPMPD, DPMPD-2,6, DPMPD-2,4 and DPMPD-2,3)

114

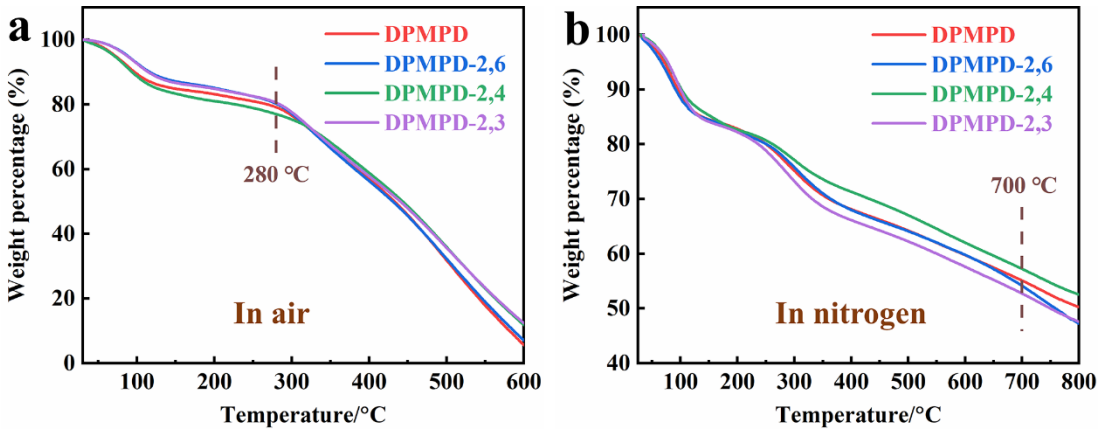

115

116 **Fig. S3** Thermogravimetric curves of DPMPD-based polymers (DPMPD, DPMPD-2,6, DPMPD-2,4 and
117 DPMPD-2,3). (a) In air, (b) In nitrogen.

118

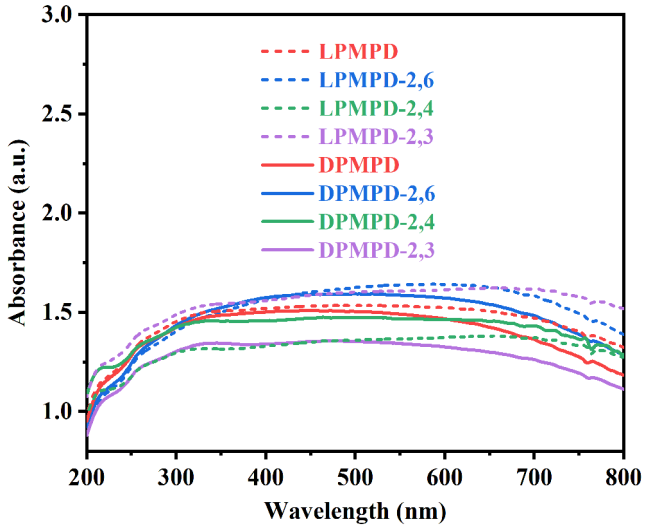

119

120 **Fig. S4** DRUV-vis spectra of LPMPD- and DPMPD-based polymers.

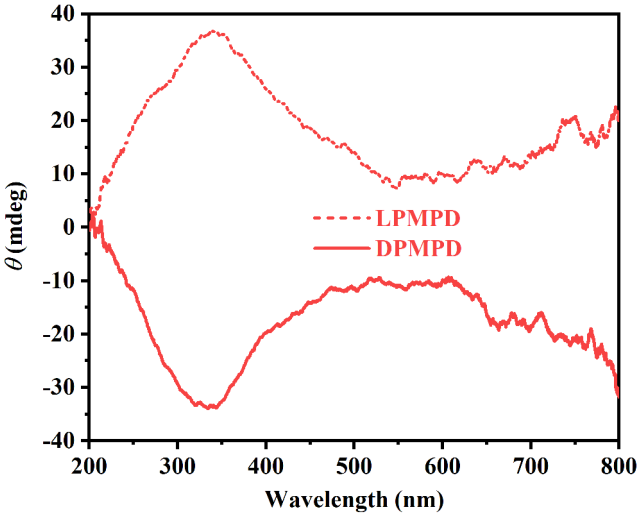

Fig. S5 DRCD spectra of LPMPD and DPMPD.

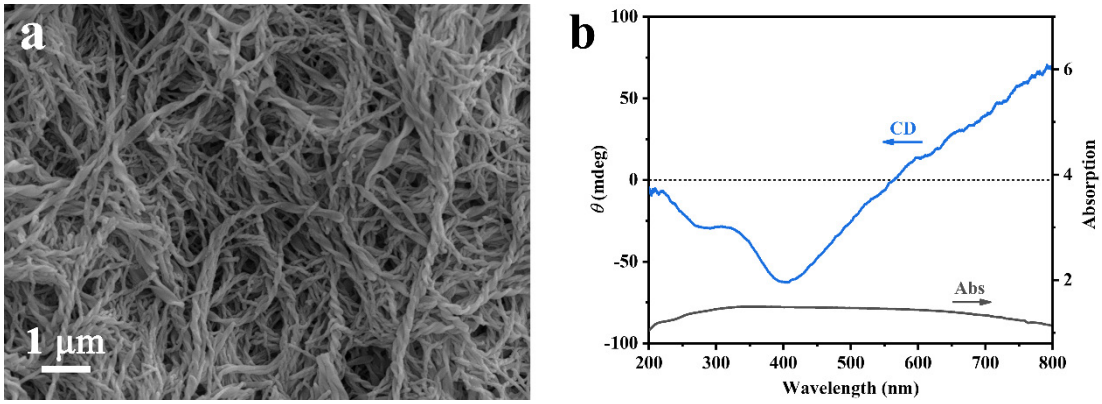

Fig. S6 (a) SEM image of DPMPD-2,6-F127. In the preparation of DPMPD-2,6, F-127 was introduced to co-assemble with D-Phg, MPD and 2,6-DAP to tune the helical senses (pitch and aspect ratio) of the resulting copolymer. (b) DRCD and DRUV-vis spectra of DPMPD-2,6-F127.

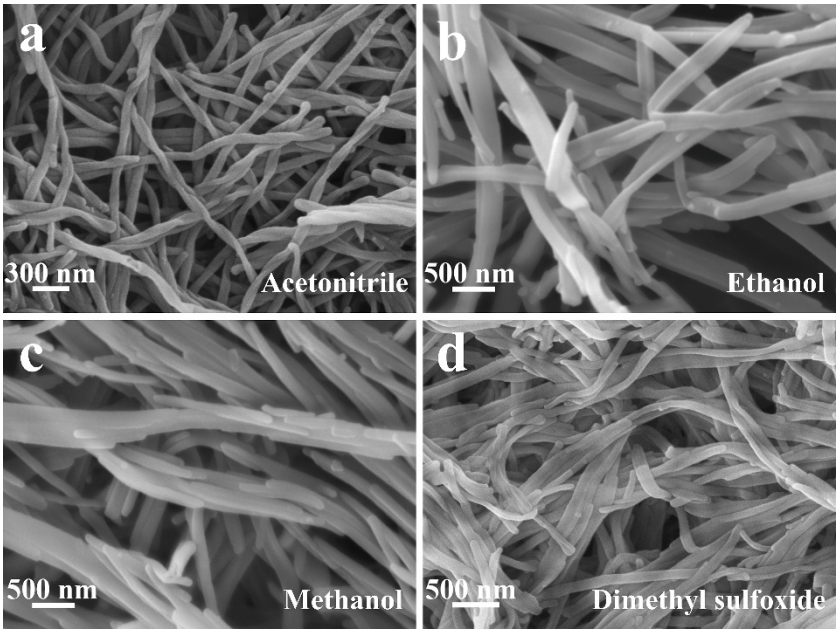

Fig. S7 SEM images of DPMPD prepared in different single good solvent systems. (a) Acetonitrile, (b) Ethanol, (c) Methanol, (d) Dimethyl sulfoxide. (The good solvent for all systems was a single component, and the poor solvent was H_2O)

As shown in Fig. S7, the microstructures of the homopolymer DPMPD obtained in different good solvent systems were distinct. As far as the effect on hydrogen bonds between water molecules, the DPMPD obtained from the cosolvent ACN (hydrogen bond maker) system had a right-handed twisted conformation (Fig. S7a), while the ethanol or methanol (hydrogen bond breaker) system yielded DPMPD only in non-twisted nanoribbons (Fig. S7b, S7c). As for the universal solvent DMSO, its system also failed to collect twisted DPMPD (Fig. S7d). Therefore, acetonitrile was indispensable for the formation of chiral homopolymer DPMPD.

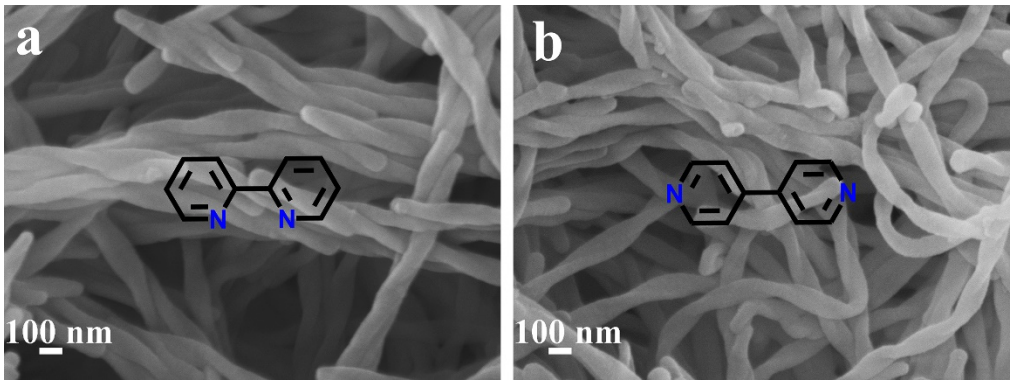

Fig. S8 SEM images of copolymers obtained by introducing bipyridines to copolymerize with MPD during the preparation of DPMPD. (a) 2,2'-bipyridine and (b) 4,4'-bipyridine. D-PhgC_{16} was used in all cases.

As shown in Fig. S8, when the introduced comonomers only contains pyridine groups, the handedness of the resulting copolymers was the same as that of the homopolymer DPMPD, both of which were right-handed. Hence, the pyridine group was not the only factor for the copolymerization-mediated handedness inversion of DPMPD.

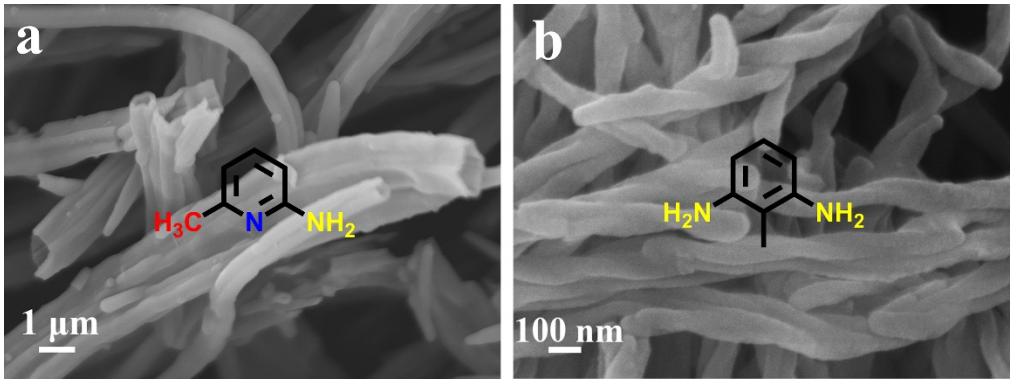

Fig. S9 SEM images of the copolymers obtained by copolymerizing (a) 2-amino-6-methylpyridine and (b) 2,6-diaminotoluene with MPD during the preparation of DPMPD. D-PhgC_{16} was used in all cases.

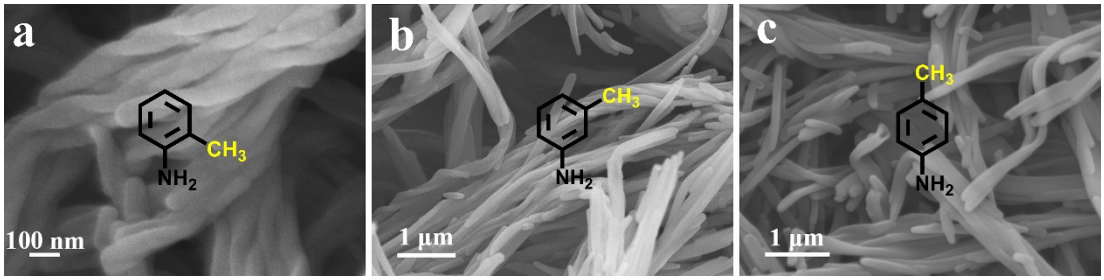

Fig. S10 SEM images of copolymers obtained by introducing methylaniline to copolymerize with MPD during the preparation of DPMPD. (a) o-methylaniline, (b) m-methylaniline and (c) p-methylaniline. D-PhgC_{16} was used in all cases.

Unlike the previously reported studies,[2] this handedness caused by methyl steric hindrance did not occur in our DPMPD system. When the methyl group was in the ortho position, the copolymer maintained the same right-handedness as the homopolymer DPMPD (Fig. S10a). By shifting the methyl group to meta position, the resulting copolymer transformed a mixture of non-twisted nanoribbons and small amounts of right-handed helices (Fig. S10b). Further turning the methyl group to para-position, the copolymers of the p-methylaniline system were completely non-twisted nanoribbons (Fig. S10c). Therefore, the mechanism of copolymerization-induced helicity inversion might be different for the two systems.

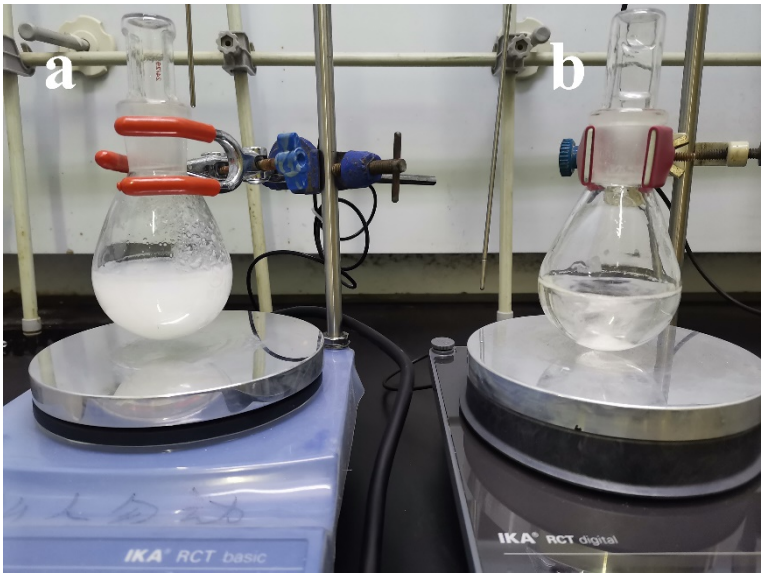

Fig. S11 Optical images of (a) MPD system and (b) 2,4-DAP system before the addition of the oxidant APS.

As exhibited in Fig. S11, MPD co-assembled with D-PhgC_{16} in a mixture solvent of DMSO, ACN and H_2O to form an opaque suspension, where the supramolecular co-assemblies could be obtained by simple filtration or centrifugation. When 2,4-DAP was further introduced, the co-assembled system transformed into a clear solution which was similar to CTAB aqueous micelles. Therefore, the D-PhgC_{16}/MPD-2,4 co-assemblies could not be collected through filtration or centrifugation for further characterizations.

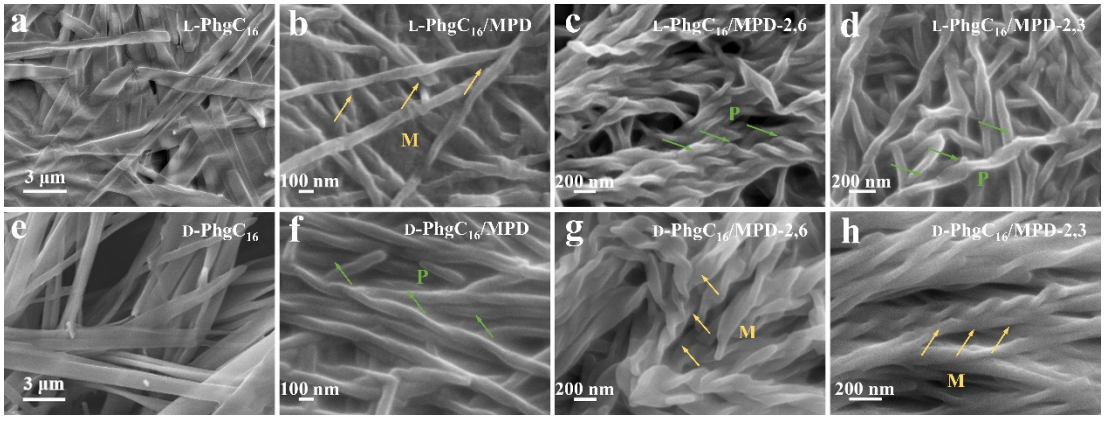

Fig. S12 SEM images (a, c, e, g, i) of L-PhgC_{16}-based dried assemblies and SEM images of (b, d, f, h, j) of D-PhgC_{16}-based dried assemblies. (M: left-handed; P: right-handed)

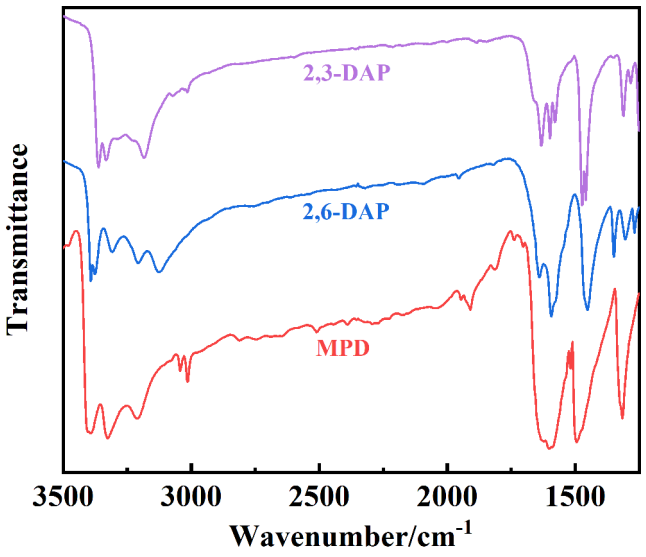

Fig. S13 FTIR spectra of the reactive monomers of MPD, 2,6-DAP and 2,3-DAP.

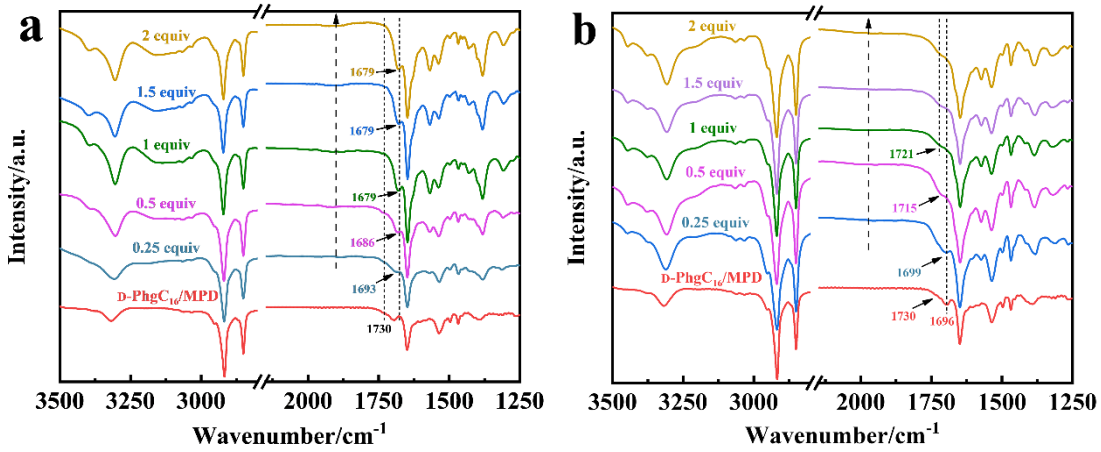

Fig. S14 FTIR spectra of (a) D-PhgC$_{16}$/MPD-2,6 and (b) D-PhgC$_{16}$/MPD-2,3 co-assemblies with different stoichiometric ratios between 2,6-DAP/2,3-DAP and D-PhgC$_{16}$. The total mass of 2,6-DAP/2,3-DAP and MPD remained constant.

In order to determine a plausible interaction stoichiometry ratio of 2,6-DAP/2,3-DAP and D-PhgC$_{16}$, we investigated the changes in the FTIR characteristic peaks of their corresponding supramolecular co-assemblies (D-PhgC$_{16}$/MPD-2,6 and D-PhgC$_{16}$/MPD-2,3) by varying the amount of 2,6-DAP/2,3-DAP. As shown in Fig. S14a, as the amount of 2,6-DAP was gradually increased from 0 to 1 molar equivalent of D-PhgC$_{16}$, the initial peak at 1696 cm^{-1} was progressively red-shifted to 1679 cm^{-1} and the intensity of the hydrogen bond peak between the carboxyl and pyridine units near 1907 cm^{-1} was also increasingly improved. After further raising the amount of 2,6-DAP, the peak at 1679 cm^{-1} and the hydrogen bond peak described above remained almost unchanged. The similar corresponding scenario also occurred in the 2,3-DAP system (Fig. S14b). As the amount of 2,3-DAP was gradually grown to 1 molar equivalent of D-PhgC$_{16}$, the initial peak at 1696 cm^{-1} progressively blue-shifted to 1721 cm^{-1} and the hydrogen bond peak between the carboxyl and pyridine units around 1982 cm^{-1} increasingly reached saturation. After

further boosting the amount of 2,3-DAP, the peak at 1721 cm^{-1} as well as the hydrogen bond peak mentioned above also remained essentially unchanged. These changes demonstrated that the hydrogen bond between 2,3-DAP and D-PhgC_{16} began to gradually replace the electrostatic interactions between MPD and D-PhgC_{16} in the D-PhgC_{16}/MPD-2,3 co-assemblies as the amount of 2,3-DAP was increased. Thus, it could be inferred that the reasonable stoichiometric ratio of 2,6/2,3-DAP and D-PhgC_{16} was 1:1.

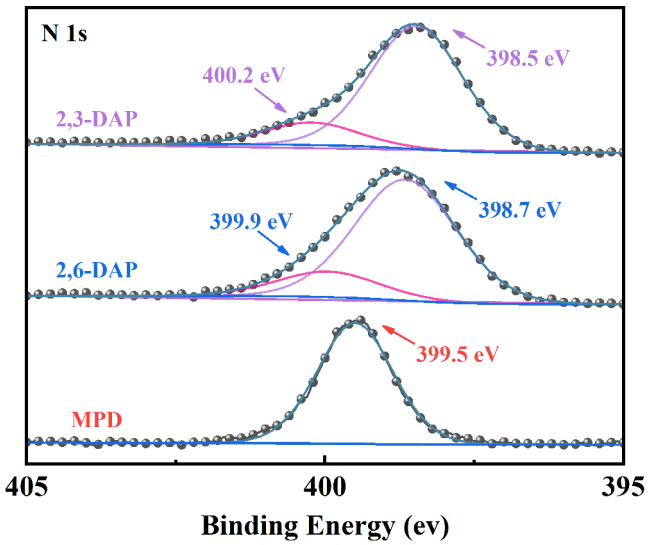

Fig. S15 High-resolution XPS N 1s spectra of the reactive monomers of MPD, 2,6-DAP and 2,3-DAP.

As shown in Fig. S15 and Fig. 4c, when the reactive monomers of MPD, 2,6-DAP and 2,3-DAP were introduced to co-assemble with D-PhgC_{16}, the characteristic peaks that were originally part of each were shifted to some extent. For D-PhgC_{16}/MPD co-assemblies, the electrostatic interaction between D-PhgC_{16} and MPD resulted in a new peak corresponding to C-NH_3^+ at 401.9 eV, while the characteristic peak of amide nitrogen overlapped with that of MPD and shifted slightly to 399.9 eV. In the case of D-PhgC_{16}/MPD-2,6 co-assemblies, the characteristic peak of 2,6-DAP at 399.9 eV was shifted to 400.5 eV due to the strong electron withdrawing effect of the carboxylate unit of D-PhgC_{16}, while another characteristic peak of 2,6-DAP overlapped with that of the amide nitrogen to form a new peak at 399.4 eV. Similarly, in the 2,3-DAP system, the characteristic peak of 2,3-DAP at 400.2 eV moved to 401.0 eV and another characteristic peak at 398.5 eV overlapped with that of the amide nitrogen, resulting in a new peak at 399.7 eV. These results also suggested the existence of interactions between these active monomers and D-PhgC_{16}, such as electrostatic interactions and hydrogen bonds.

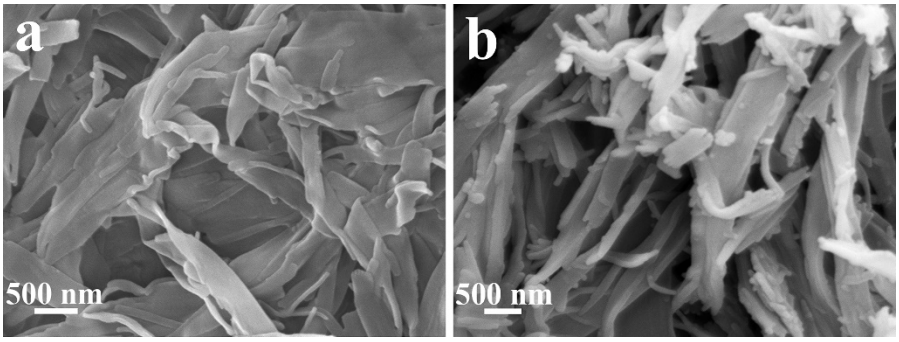

Fig. S16 SEM images of (a) homopolymer PMPD and (b) copolymer PMPD-2,6 obtained in the racemic-PhgC_{16} system. Racemic-PhgC_{16} was composed of L-PhgC_{16} and D-PhgC_{16} in a 1:1 molar ratio.

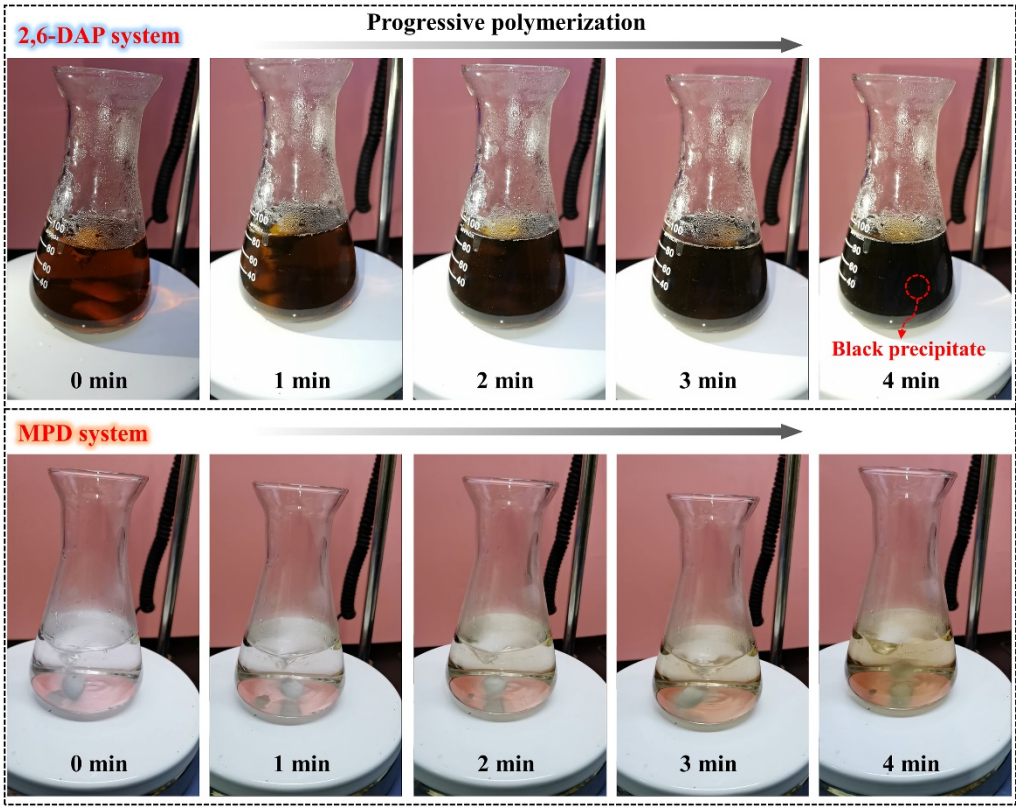

Fig. S17. Optical images of the self-polymerizing systems of 2,6-DAP and MPD taken at different time points. The initial reaction concentrations of 2,6-DAP and MPD as well as the corresponding amounts of oxidant APS used were controlled to be equal. Both 2,6-DAP and MPD were first dissolved under heating conditions and then naturally cooled to room temperature before adding APS, using a mixture of DMSO and H_2O as the solvent.

The difference in the self-polymerization rate of 2,6-DAP and MPD could be clearly observed in Fig. S17. For the 2,6-DAP system, when APS was added, the reaction system changed from burgundy to dark brown within 2 minutes and some black solid precipitates appeared within 4 minutes. However, for the MPD system, the reaction mixture only turned from colourless to light yellow 2 minutes after the addition of APS. Even after 4 minutes of self-polymerization, the colour of the system remained clear pale yellow, and no solid products occurred. Thus, the self-polymerization of 2,6-DAP was much faster than that of MPD.

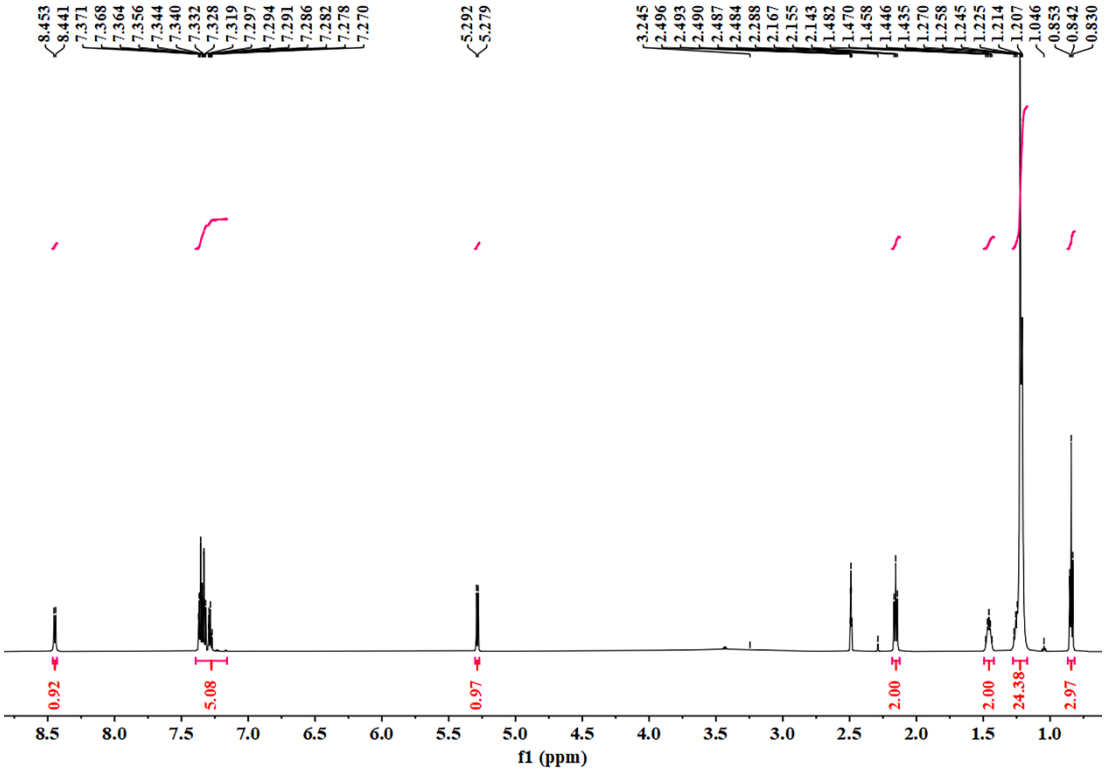

Fig. S18 The ^{1}H NMR spectra of D-PhgC_{16} in DMSO-d_6.

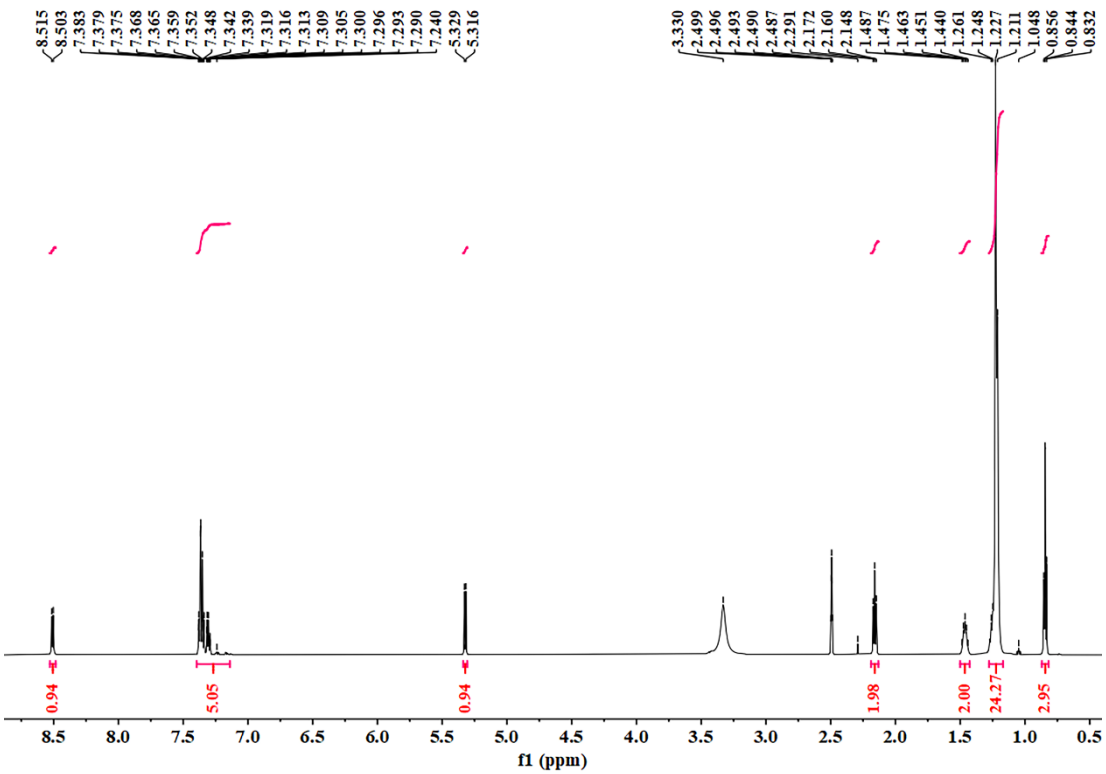

Fig. S19 The ^{1}H NMR spectra of L-PhgC_{16} in DMSO-d_6.

Table S1. Atom sites of modelled D-PhgC_{16}/2,6-DAP

Atom site label	Atom site fract X	Atom site fract Y	Atom site fract Z
C	-4.871339	1.952541	-1.695597
C	-4.37592	0.5623	-2.106248
C	-2.075255	-0.208811	-2.576119
C	-0.717852	0.194631	-3.136233
H	-0.813442	1.049133	-3.818258
H	-0.34853	-0.65391	-3.723246
C	0.287927	0.52281	-2.016324
H	0.338815	-0.330035	-1.328354
H	-0.085652	1.374394	-1.430333
C	1.688901	0.841825	-2.552591
H	1.629008	1.68568	-3.255985
H	2.054989	-0.01553	-3.136428
C	2.700981	1.172249	-1.447818
H	2.746837	0.333957	-0.73716
H	2.342684	2.038849	-0.872697
C	4.110663	1.461281	-1.979859
H	4.06747	2.30147	-2.688939
H	4.462765	0.594329	-2.558629
C	5.129754	1.778833	-0.877834
H	5.162292	0.942494	-0.163666
H	4.786789	2.653299	-0.305041
C	6.543996	2.042562	-1.41083
H	6.514908	2.883555	-2.119703
H	6.880019	1.169756	-1.990583
C	7.5705	2.341654	-0.310575
H	7.594554	1.501519	0.399628
H	7.240378	3.217565	0.2676
C	8.986415	2.590884	-0.846133
H	9.309768	1.71826	-1.433365
H	8.965533	3.437347	-1.548754
C	10.019874	2.869488	0.252936
H	10.040955	2.020935	0.953239
H	9.698303	3.740776	0.842829
C	11.435303	3.11599	-0.285153
H	11.75143	2.248455	-0.883779
H	11.416693	3.970792	-0.977694
C	12.474156	3.376329	0.813066
H	12.496999	2.518232	1.50188
H	12.157824	4.24023	1.416791
C	13.88824	3.627831	0.273941
H	14.202293	2.76664	-0.333187

H	13.867075	4.488876	-0.409298
C	14.92157	3.876972	1.377336
H	14.994014	3.016177	2.053938
H	15.918925	4.056621	0.959853
H	14.651837	4.750561	1.98374
O	-5.899856	1.898893	-0.879927
N	-3.054751	0.723113	-2.69001
H	-2.835631	1.655186	-3.020233
O	-2.253386	-1.306281	-2.039617
C	-4.608793	-2.048947	1.538696
C	-4.059636	-3.375191	1.003923
C	-1.700817	-3.875808	0.61914
C	-0.468979	-3.607109	-0.237795
H	-0.650455	-2.785928	-0.938509
H	-0.307871	-4.512829	-0.839707
C	0.77529	-3.351757	0.626032
H	0.639265	-2.417472	1.190156
H	0.848466	-4.153539	1.369855
C	2.070763	-3.270443	-0.189972
H	1.975556	-2.487522	-0.957917
H	2.214771	-4.213987	-0.737301
C	3.309556	-2.986307	0.669381
H	3.164267	-2.039255	1.210766
H	3.400271	-3.76421	1.441645
C	4.61502	-2.913344	-0.133316
H	4.517522	-2.146256	-0.916603
H	4.771888	-3.865864	-0.660949
C	5.845321	-2.600642	0.728308
H	5.683716	-1.648799	1.256627
H	5.944621	-3.367061	1.511287
C	7.153508	-2.518369	-0.069001
H	7.050222	-1.758167	-0.858009
H	7.323908	-3.472842	-0.588927
C	8.376281	-2.185523	0.795803
H	8.200321	-1.233601	1.319351
H	8.483027	-2.947359	1.582357
C	9.685832	-2.089457	0.002406
H	9.577217	-1.329309	-0.78586
H	9.866795	-3.041622	-0.518248
C	10.903375	-1.746662	0.870699
H	10.717765	-0.79737	1.395612
H	11.015524	-2.509139	1.655899
C	12.213277	-1.637759	0.079607
H	12.100543	-0.874415	-0.705001

H	12.400721	-2.586179	-0.445688
C	13.428377	-1.292245	0.949928
H	13.239885	-0.344688	1.477184
H	13.543788	-2.05619	1.73343
C	14.738554	-1.177252	0.160233
H	14.62362	-0.412776	-0.621687
H	14.927816	-2.123484	-0.36654
C	15.945877	-0.831312	1.037791
H	16.865078	-0.758877	0.445178
H	15.802615	0.129397	1.548112
H	16.106446	-1.594054	1.809807
O	-5.206716	-2.179958	2.714481
O	-1.683648	-4.692548	1.537198
N	-2.822132	-3.160532	0.28633
H	-2.7746	-2.445475	-0.436408
H	-3.801561	-4.00149	1.861278
O	-4.351035	2.981701	-2.120083
O	-4.526507	-0.987031	0.931777
H	-4.29234	-0.052022	-1.205219
C	-5.397251	-0.077086	-3.049257
C	-6.327638	-0.991466	-2.54758
C	-5.443033	0.275	-4.402973
C	-7.287941	-1.553474	-3.39
H	-6.291717	-1.269856	-1.498745
C	-6.402573	-0.286509	-5.245252
H	-4.720304	0.982073	-4.801372
C	-7.328563	-1.20189	-4.7401
H	-7.994682	-2.274574	-2.989163
H	-6.427108	-0.008708	-6.295853
H	-8.074926	-1.641059	-5.396923
C	-5.15354	-4.085058	0.193972
C	-6.245789	-4.653297	0.864365
C	-5.088569	-4.178133	-1.199246
C	-7.250707	-5.308657	0.154572
H	-6.304798	-4.581925	1.947119
C	-6.095175	-4.836934	-1.909902
H	-4.248076	-3.74362	-1.730788
C	-7.177664	-5.40421	-1.237311
H	-8.087088	-5.751494	0.689316
H	-6.029017	-4.903063	-2.992546
H	-7.956866	-5.921203	-1.791408
H	-6.269737	2.832282	-0.631359
H	-5.532242	-1.269815	3.059605
C	-8.189308	4.015314	0.594422

C	-9.073099	5.083193	0.827626
C	-8.704173	6.345613	0.375681
C	-7.4942	6.541355	-0.278005
C	-6.661398	5.424248	-0.477161
H	-10.011488	4.914783	1.345589
H	-9.368253	7.190399	0.541042
H	-7.187304	7.521233	-0.628663
N	-8.498298	2.731074	0.974519
H	-7.720502	2.097915	1.155749
H	-9.258354	2.636862	1.633661
N	-5.434231	5.543554	-1.074402
H	-5.275417	6.381189	-1.615537
H	-5.002797	4.697794	-1.448719
N	-7.01151	4.188038	-0.050617
C	-6.006229	-0.128943	5.318189
C	-6.164298	0.931059	6.226531
C	-6.191468	2.223976	5.714483
C	-6.070315	2.451449	4.347628
C	-5.91697	1.33591	3.507495
H	-6.260571	0.736363	7.289568
H	-6.306636	3.066783	6.391253
H	-6.090722	3.453064	3.931253
N	-6.004903	-1.443315	5.73456
H	-5.620366	-2.121646	5.088387
H	-5.772387	-1.613152	6.702701
N	-5.842163	1.466128	2.133846
H	-5.499432	2.358379	1.798839
H	-5.436779	0.672168	1.632874
N	-5.888706	0.077824	3.991104

Table S2. Atom sites of modelled D-PhgC_{16}/MPD

Atom site label	Atom site fract X	Atom site fract Y	Atom site fract Z
C	-4.900256	1.443943	-1.450904
C	-4.38997	0.133203	-2.049298
C	-2.036908	-0.423616	-2.602388
C	-0.776385	0.080078	-3.296514
H	-0.981069	0.998597	-3.861128
H	-0.488409	-0.687267	-4.02603
C	0.385229	0.310448	-2.31536
H	0.567048	-0.618329	-1.76179
H	0.090717	1.064862	-1.572264
C	1.671555	0.758509	-3.020653
H	1.47733	1.683664	-3.583719
H	1.956434	0.002542	-3.767313
C	2.844097	0.987371	-2.058553
H	3.033487	0.062591	-1.493807
H	2.561238	1.74543	-1.313259
C	4.136599	1.422715	-2.761379
H	3.953774	2.355224	-3.316026
H	4.409824	0.669857	-3.515616
C	5.314939	1.624886	-1.800171
H	5.488769	0.692461	-1.242239
H	5.045879	2.381546	-1.048185
C	6.615548	2.042965	-2.498211
H	6.450215	2.983589	-3.044565
H	6.875839	1.29223	-3.259178
C	7.796501	2.215361	-1.534265
H	7.953767	1.274722	-0.985034
H	7.539535	2.969188	-0.775185
C	9.104839	2.618417	-2.226566
H	9.355787	1.869109	-2.992079
H	8.954449	3.564955	-2.766996
C	10.286257	2.768022	-1.259332
H	10.430985	1.821389	-0.716922
H	10.037421	3.519317	-0.495037
C	11.60024	3.160699	-1.946853
H	11.845793	2.411929	-2.714684
H	11.459804	4.110568	-2.484173
C	12.781325	3.296787	-0.977472
H	12.919731	2.346913	-0.438765
H	12.537953	4.046796	-0.209958
C	14.098739	3.683656	-1.661612
H	14.341335	2.93483	-2.429077

H	13.962885	4.634009	-2.197448
C	15.272108	3.811692	-0.684825
H	15.454222	2.866247	-0.158393
H	16.197864	4.087107	-1.203044
H	15.074374	4.57867	0.074249
O	-5.929594	1.267257	-0.624805
N	-3.113382	0.401175	-2.694789
H	-2.988921	1.342919	-3.04391
O	-2.062118	-1.508502	-2.014858
C	-4.486832	-2.460493	1.310162
C	-3.678906	-3.725966	1.010391
C	-1.254149	-3.974218	0.846606
C	0.018556	-3.527819	0.133846
H	-0.171904	-2.64401	-0.485161
H	0.295329	-4.339367	-0.55447
C	1.166724	-3.293643	1.125494
H	0.909018	-2.454257	1.787179
H	1.246171	-4.177629	1.768499
C	2.511424	-3.012562	0.445484
H	2.421736	-2.123043	-0.19696
H	2.76172	-3.847192	-0.2265
C	3.658942	-2.802789	1.44233
H	3.40142	-1.977965	2.12334
H	3.754706	-3.697787	2.074466
C	5.008333	-2.504648	0.776196
H	4.91266	-1.60313	0.151737
H	5.263859	-3.323794	0.087559
C	6.155499	-2.306523	1.775622
H	5.8918	-1.49919	2.475051
H	6.263164	-3.214024	2.388143
C	7.499698	-1.980279	1.111876
H	7.391484	-1.068293	0.505084
H	7.762008	-2.783177	0.406833
C	8.648158	-1.788193	2.110872
H	8.38002	-0.994133	2.823669
H	8.765805	-2.704251	2.708759
C	9.987257	-1.440602	1.4476
H	9.869205	-0.521282	0.853949
H	10.254076	-2.231382	0.730649
C	11.137198	-1.252981	2.445671
H	10.867253	-0.467195	3.166886
H	11.260465	-2.174358	3.034228
C	12.4733	-0.893474	1.782726
H	12.350227	0.030461	1.197329

H	12.741931	-1.676969	1.058447
C	13.624401	-0.710091	2.779959
H	13.355819	0.071904	3.505993
H	13.750079	-1.634339	3.363779
C	14.959869	-0.346685	2.11809
H	14.835579	0.579039	1.537434
H	15.227769	-1.12674	1.391182
C	16.10415	-0.169212	3.121331
H	17.042687	0.08994	2.617945
H	15.880606	0.628559	3.840451
H	16.275952	-1.089652	3.693042
O	-5.465729	-2.667903	2.18554
O	-1.239868	-4.831281	1.726975
N	-2.405408	-3.364549	0.430062
H	-2.375898	-2.625155	-0.268062
H	-3.462627	-4.230656	1.95648
O	-4.422408	2.534884	-1.724904
O	-4.273291	-1.382695	0.774661
H	-4.214323	-0.565926	-1.22867
C	-5.430559	-0.45584	-3.001614
C	-5.977629	-1.716521	-2.750533
C	-5.843632	0.254627	-4.136278
C	-6.919561	-2.265791	-3.622954
H	-5.658028	-2.27637	-1.877032
C	-6.7856	-0.291276	-5.006988
H	-5.428286	1.23947	-4.338528
C	-7.325843	-1.554767	-4.752447
H	-7.325852	-3.252656	-3.417967
H	-7.099168	0.269371	-5.88381
H	-8.0581	-1.981231	-5.433045
C	-4.520383	-4.672347	0.140968
C	-5.491336	-5.488093	0.735569
C	-4.344495	-4.725306	-1.246114
C	-6.271105	-6.343657	-0.041749
H	-5.634423	-5.45058	1.811848
C	-5.127077	-5.582181	-2.024783
H	-3.587623	-4.105369	-1.717462
C	-6.091839	-6.393356	-1.426261
H	-7.013597	-6.978242	0.435406
H	-4.975057	-5.616713	-3.100533
H	-6.69468	-7.065175	-2.031857
N	-6.2887	3.708677	0.494542
H	-5.507208	4.101251	-0.027338
N	-6.899473	-0.285643	1.966441

H	-7.893855	-0.432405	1.813694
C	-7.467818	4.501757	0.411276
C	-8.439599	4.397354	1.409443
C	-7.678356	5.332132	-0.696191
C	-9.633558	5.127926	1.318001
H	-8.265583	3.745614	2.263747
C	-8.867236	6.055566	-0.78102
H	-6.92529	5.403334	-1.476175
C	-9.842298	5.964601	0.208438
H	-9.036826	6.703577	-1.63698
H	-10.761342	6.540204	0.130984
C	-6.637817	0.732308	2.920493
C	-7.605725	1.0862	3.865144
C	-5.375462	1.346961	2.942961
C	-7.332118	2.053578	4.847672
H	-8.576364	0.592488	3.853712
C	-5.114705	2.315817	3.913051
H	-4.616868	1.039291	2.230221
C	-6.07375	2.680649	4.855952
H	-4.137061	2.790794	3.94096
H	-5.848523	3.42948	5.610775
H	-5.999518	3.517677	1.45315
H	-6.444176	-0.094957	1.071846
H	-6.200139	2.177292	-0.250009
H	-6.012901	-1.822626	2.241757
N	-10.577024	5.065583	2.350797
H	-11.519936	5.308047	2.071374
H	-10.565437	4.200931	2.877913
N	-8.275583	2.34607	5.832259
H	-8.186336	3.256295	6.265182
H	-9.236103	2.125468	5.60378

References

1. Zha X. L. et al. Handedness Inversion of Chiral 3-Aminophenol Formaldehyde Resin Nanotubes Mediated by Metal Coordination. *Angew. Chem. Int. Ed.* **60**, 7759-7769 (2021).

2. Yan Y., Deng K., Yu Z. & Wei Z. X. Tuning the supramolecular chirality of polyaniline by methyl substitution. *Angew. Chem. Int. Ed.* **48**, 2003-2006 (2009).